Supplementary Information (SI) for Nanoscale.

Supplementary Information for

Interfacial Polarization-Induced Tribological Behavior in MoS_2/β-Te and G/β-Te Heterostructures

Guoliang Ru[1], Weihong Qi[1,2]*, Kaiyuan Xue[1], Mengzhao Wang[1], Xuqing Liu[1]

[1] State Key Laboratory of Solidification Processing and Center of Advanced Lubrication and Seal Materials, Northwestern Polytechnical University, Xi'an 710072, China

[2] Shandong Laboratory of Yantai Advanced Materials and Green Manufacturing, Yantai 265503, China

[3] State Key Laboratory of Solid Lubrication, Lanzhou Institute of Chemical Physics, Chinese Academy of Sciences, Lanzhou 730000, China

*Correspondence should be addressed to qiwh216@nwpu.edu.cn (Weihong Qi)

Supplementary Figures

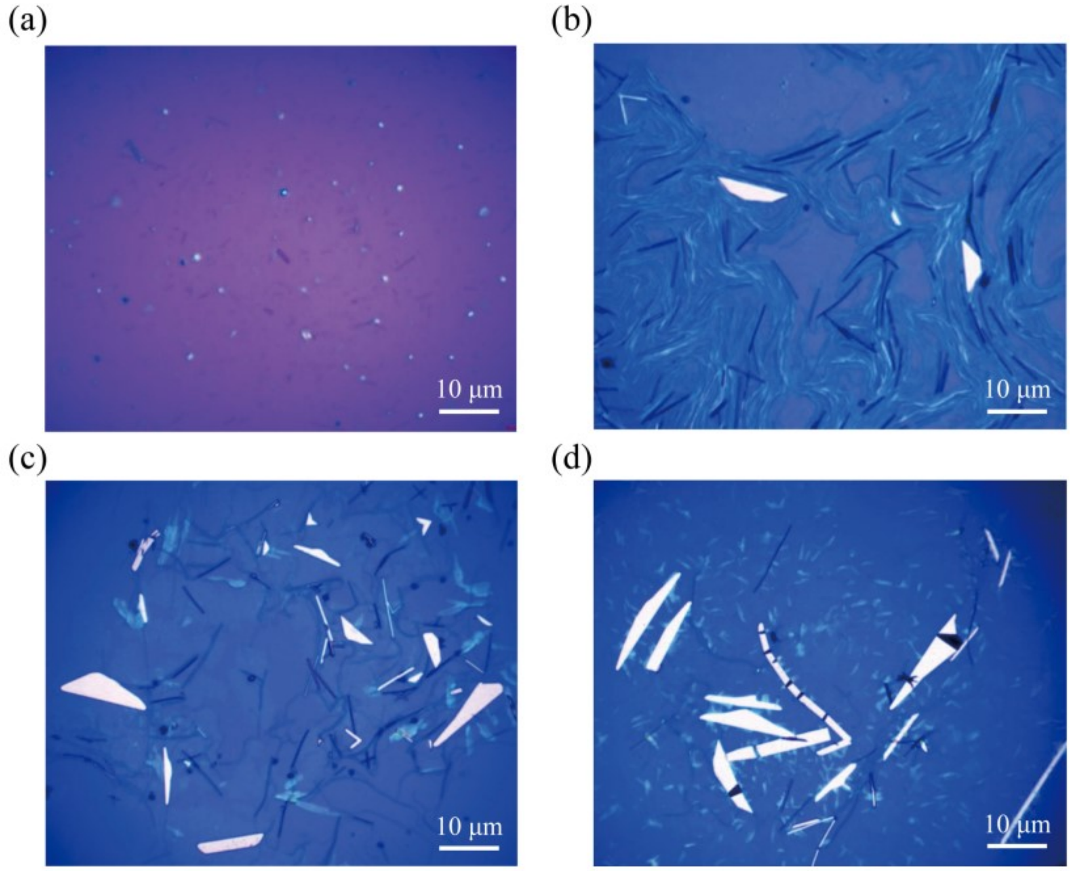

Supplementary Figure 1. Optical microscope images showing the evolution of the tellurium crystal morphology and distribution after different reaction times: (a) 10 h, (b) 15 h, (c) 20 h, and (d) 25 h. All scales are 10 µm.

During the initial 10-hour reaction period, no formation of layered tellurium was observed, with only the presence of some flocculent nanowires detected. Upon extending the reaction time to 15 hours, minute quantities of tellurium structures began to emerge. As the reaction duration was further prolonged to 20–25 hours, a significant increase in both the quantity and size of tellurium structures was readily discernible, with dimensions evolving from less than 10 micrometres initially to approximately 30 micrometres ultimately. Notably, consistent coexistence of nanowires with tellurene was observed throughout the entire reaction process.

These observations clearly demonstrate that the reaction time serves as a critical parameter in controlling both the size and yield of tellurium structures. As the reaction time increased, we observed a marked increase in both the lateral dimensions and production yield of the tellurium structures. This finding provides crucial experimental evidence for precise control over the synthesis of two-dimensional tellurium materials while simultaneously laying a foundation for a deeper understanding of their growth mechanisms.

(a) (b)

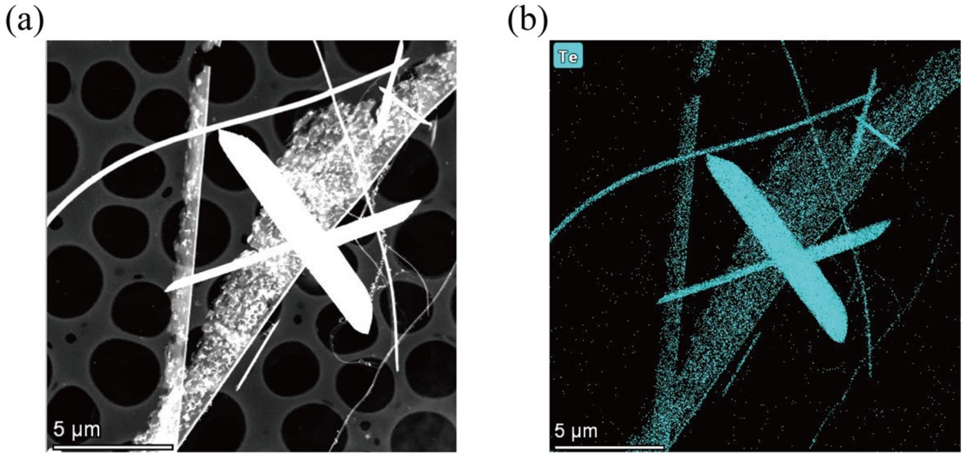

Supplementary Figure 2. Energy-dispersive X-ray spectroscopy (EDS) characterization of tellurium nanostructures. (a) Image showing the morphology of the synthesized sample. (b) Elemental distribution map obtained from EDS analysis. The corresponding EDS spectrum revealed the exclusive presence of tellurium without detectable impurities, confirming the high purity and quality of the synthesized material.

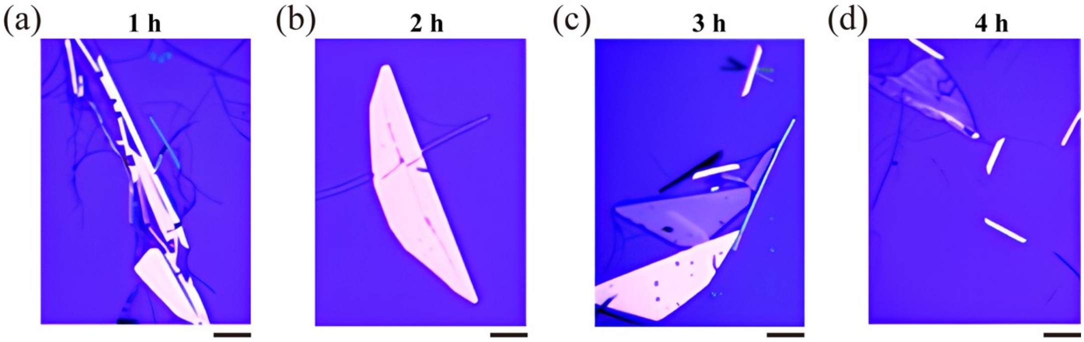

Supplementary Figure 3. Time-dependent thinning of 2D tellurene crystals in acetone. Optical microscopy images showing the progressive reduction in thickness of tellurium nanostructures over time when exposed to acetone: (a) 1 h, (b) 2 h, (c) 3 h, (d) 4 h. Scale bars: 4 μm.

(a) (b)

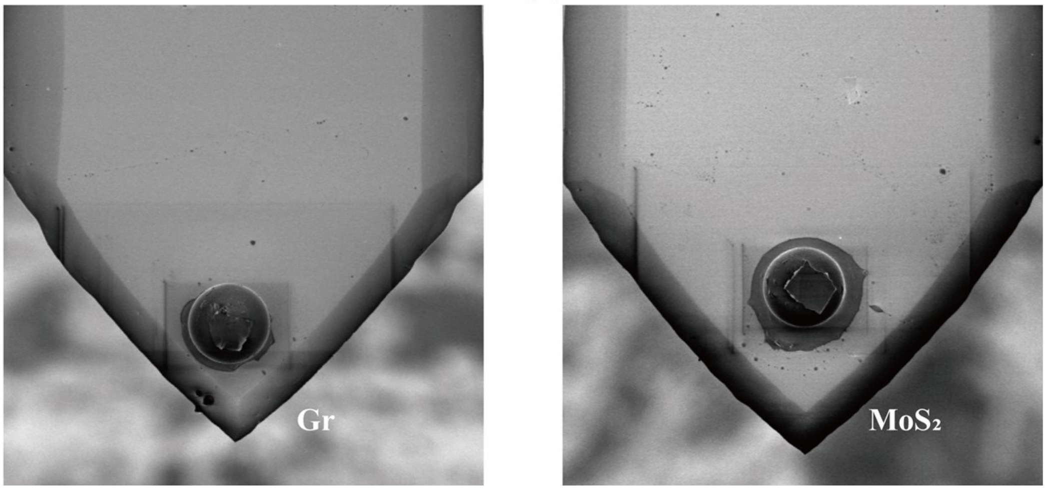

Supplementary Figure 4. Functionalized spherical colloidal probes for friction measurements. Scanning electron microscopy (SEM) images of spherical colloidal probes coated with (a) graphene and (b) MoS_2.

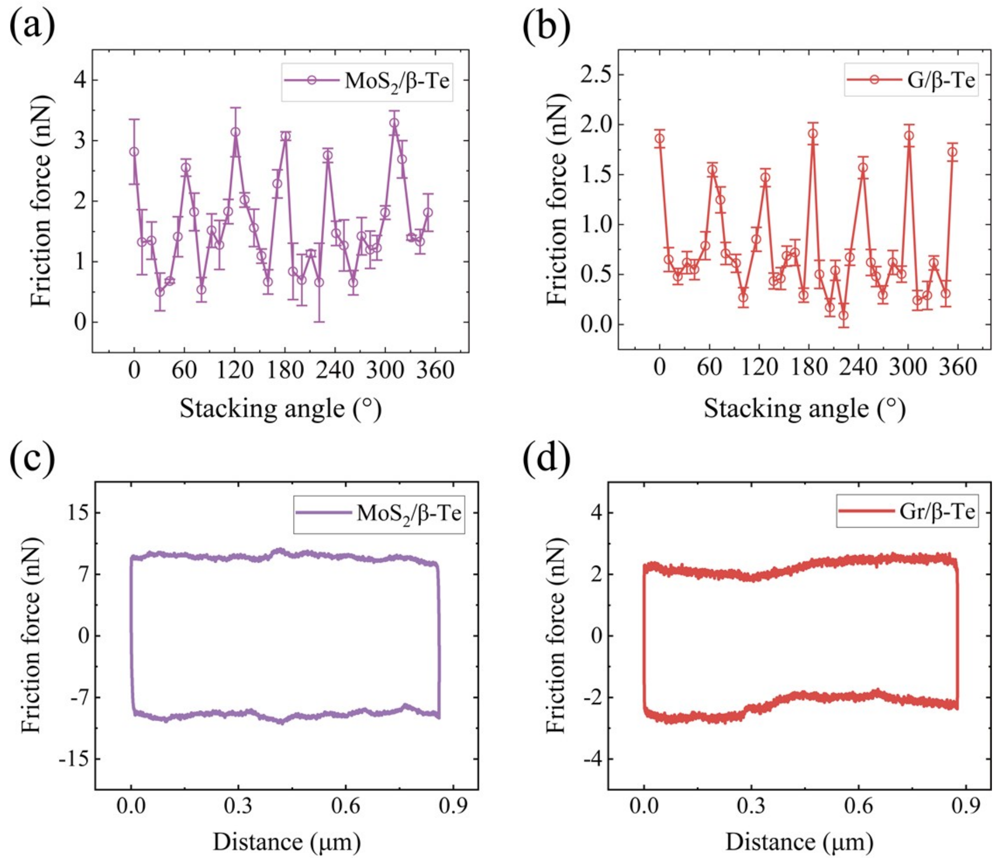

Supplementary Figure 5. Angular dependence of friction in tellurene-based van der Waals heterostructures. Friction force maps as a function of stacking angle for MoS_2/β-Te (a) and G/β-Te (b). Representative friction loops measured by atomic force microscopy (AFM) for the MoS_2/β-Te (c) and G/β-Te (d) systems.

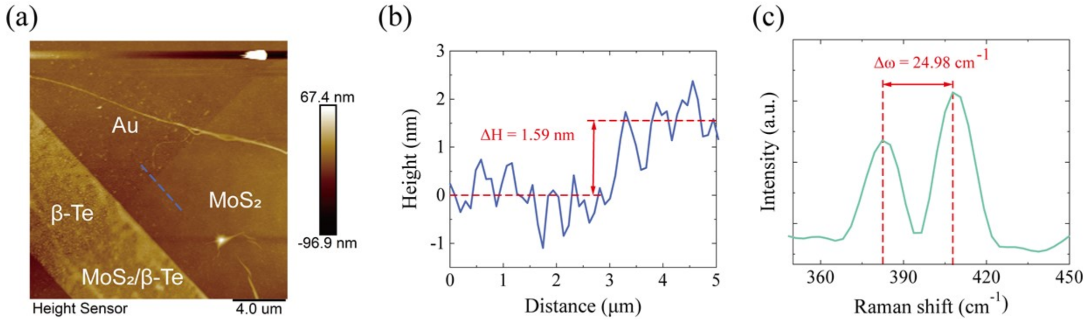

Supplementary Figure 6. Characterization of the thin layer thickness of MoS_2. (a) AFM height image, with the dashed line indicating the position where the height profile was measured. (b) Height profile extracted along the dashed line in (a). The measured thickness of the MoS_2 layer is 1.59 nm, corresponding to the typical thickness of bilayer MoS_2. (c) Raman spectrum of MoS_2, showing the frequency difference ($\Delta\omega$ = 24.98 cm^{-1}) between the E_{2g} and A_{1g} characteristic peaks, further confirming the bilayer nature of MoS_2.

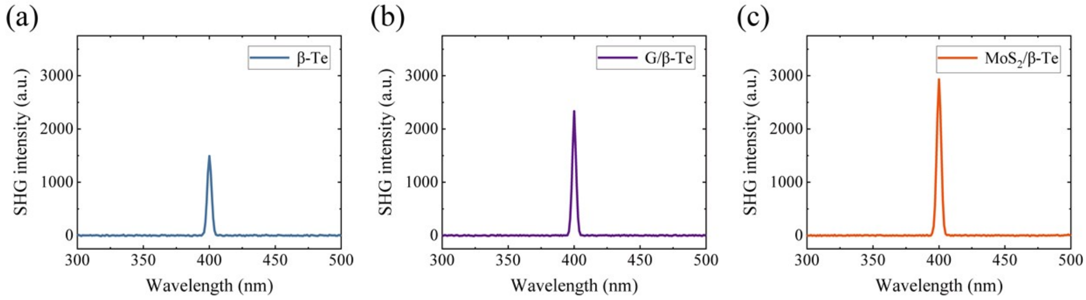

Supplementary Figure 7. Second-harmonic generation (SHG) intensity spectra. (a) SHG spectrum of β-Te. (b) SHG spectrum of the G/β-Te heterostructure. (c) SHG spectrum of the vertically stacked MoS_2/β-Te heterostructure.

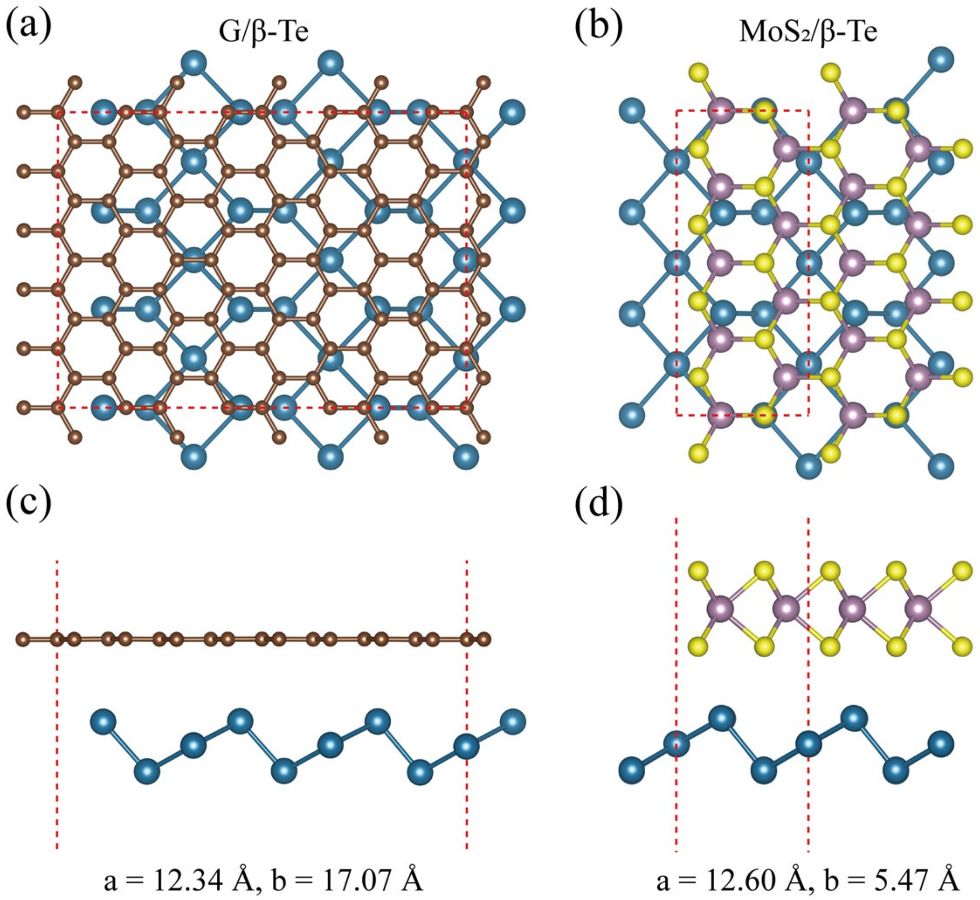

Supplementary Figure 8. Crystal structures of the tellurene-based van der Waals heterostructures. Top view (a) and side view (b) of the G/β-Te model. Top view (c) and side view (d) of the MoS_2/β-Te heterostructure model. These atomic configurations represent the structural basis for first-principles calculations of electronic properties.